**ORIGINAL ARTICLE**

CrossMark

# Europium containing red light-emitting fibers made by electrohydrodynamic casting

Yong X. Gan[1] · Niousha Panahi[2] · Christina Yu[2] · Jeremy B. Gan[3] · Wanli Cheng[4]

## Abstract

Red light-emitting polymeric micro- and nanofibers were made by electrohydrodynamic co-casting of two fluids. One fluid contains a 10 wt% concentration europium (III) complex dissolved in a dimethylformamide (DMF) solvent. The europium complex, an $Eu^{3+}$ compound with the nominal formula of $Eu(BA)_3phen/PAN$, consists of polyacrylonitrile (PAN), 1,10-phenanthroline (phen), and benzoic acid (BA). The other fluid consists of iron metal oxide nanoparticles dispersed in a solution containing 10 wt% polyacrylonitrile polymer in DMF solvent. The two fluids were electrohydrodynamically co-cast onto a soft tissue paper using a stainless steel coaxial nozzle. The intensity of the electric field used for the co-casting was 1.5 kV/cm. Scanning electron microscopic observation on the fibers obtained from the co-casting was made. The size of the fibers ranges from several hundreds of nanometers to several microns. Energy dispersive X-ray spectroscopic analysis of the fibers confirmed that the major elements included C, O, Fe, and Eu. The fluorescence of the two types of fibers was tested under the excitation of a UV light source. It was found that when the europium complex-containing solution was the sheath fluid and the iron-containing solution was the core, the prepared fibers showed red light-emitting behavior under ultraviolet light. Time-dependent fluorescence shows the two-stage decaying behavior. The first stage lasts about 2000 s and the intensity of fluorescence decreases linearly. The second stage reveals the slow decaying behavior and it lasts longer than 3 h. Based on the bi-exponential data fitting using a processing MATLAB code, the fluorescence-related constants were extracted. A bi-exponential formula was proposed to describe the time-dependent fluorescence behavior of the fiber made by the europium complex-containing solution as the sheath fluid. The decaying in the fluorescence shows two different stages. The first stage lasts about 2000 s and it is characterized by a fast decaying model. The intensity of fluorescence decreases linearly. The second stage has a slow decaying feature. It takes over 3 h for the fluorescence to die out completely. Bi-exponential data fitting shows that the time constant for the decay of fluorescence is about 10,000 s.

**Keywords** Electrohydrodynamic co-casting · Europium complex · Polyacrylonitrile fiber · Luminescence · Red light emission

✉ Yong X. Gan
  yxgan@cpp.edu

[1] Department of Mechanical Engineering, California State Polytechnic University Pomona, 3801 W Temple Avenue, Pomona, CA 91768, USA

[2] Department of Natural, Physical and Health Sciences, Citrus College, 1000 W Foothill Blvd, Glendora, CA 91741, USA

[3] Diamond Bar High School, 21400 Pathfinder Road, Diamond Bar, CA 91765, USA

[4] Troy High School, 2200 Dorothy Ln, Fullerton, CA 92831, USA

## Introduction

Electrohydrodynamic (EHD) co-casting or co-spinning uses a coaxial needle to inject a core fluid and a shell fluid at the same time under the actions of both mechanical and electric forces [1–3]. The mechanical force is mainly from the fluidic pressure generated by a syringe pump. The electric force is due to the high DC voltage applied between the coaxial needle and the ground. The EHD co-casting has been reported mainly for making organic core–shell bioactive and/or biodegradable nanofibers [4–6]. There are also many other new structures and materials prepared by this approach, including multiple compartment microcapsules [7] and hollow fibers [8–11].

Springer

The EHD co-casting using photosensitive substances for fabricating micro- and/or nanofibers has recently been studied. For example, nanofibers with a photosensitive epoxy shell and an ethylene glycol core were manufactured [12]. In addition to produce the epoxy photosensitive sheath, many researchers have studied the formation of the photosensitive titanium dioxide shell layer using metal organic compounds as the starting materials in the EHD co-casting process [13, 14].

Light-emitting polymers have been studied extensively and found applications in optoelectronics. Various polymers, including the cyanovinylene polymer derived from 3,4-dialkoxy thiophene, polyfluorene copolymers (PFO-DBT), tetraarylsilyl, poly(1,4-phenylene vinylene) (PPV), poly(1,4-phenylene) (PPP), and poly(2,5-pyridinevinylene), are reported. Several issues still remain to be addressed for such materials. Their quantum efficiencies are relatively low. The stability in air is not so good. Therefore, it is necessary to explore metal–organic complexes as the new light emission materials.

In this work, the EHD co-casting technique was used to make red light-emitting micro- and nanofibers using a europium organic complex as the functional component. The fibers consist of both europium complex layer and iron oxide-containing layer. Polyacrylonitrile (PAN) was used as the host polymer for both the shell and core layers because of its good spinnability [15, 16]. Although the basic composition of the $Eu^{3+}$ complex was similar to that from the literature [17, 18], the polymer used in this study has different structures and properties. In [17] and [18], a biodegradable polymer, polyvinyl pyrrolidone (PVP), was used.

In view of the applications of the $Eu^{3+}$ complexes, earlier studies have shown that one of the important uses is for improving the solar energy harvesting efficiency of silicon panels [19]. The main reason is that the intensive emission of $Eu^{3+}$ complexes at 612 nm matches the wavelength for generating the maximum quantum efficiency by crystalline silicon (c-Si)-based solar cells [19]. Another application is for the DNA detection [20]. A europium (III) complex was attached to carbon nanotubes for label-free and time-resolved luminescent assay of lysozyme (LYS) because of the exceptional quenching capability of carbon nanotubes for the proximate luminescent $Eu^{3+}$ complex and different propensities of single-stranded DNA and the DNA/protein complex to adsorb on carbon nanotubes [21]. In this work, the $Eu^{3+}$ complex has been studied for different applications. The objective of this work is to explore new sensors with the working mechanism of color, or fluorescence changes when chemical molecules are introduced to the sensors as mentioned in [22].

Since PVP is a water-soluble polymer, it loses the function as a binding agent in moisture. Therefore, PAN is selected in this study. Scanning electron microscopic analysis of the morphology and the composition was performed. The photoluminescence of the prepared fibers under ultraviolet light excitation was characterized. The lifetime of the luminescence was estimated by the time-dependent photoluminescence intensity test.

Comparison on the ultraviolet light sensitivity of the two fibers (one with a europium shell, the other with an iron shell) was made as well. It is found that the fiber with an iron oxide-containing shell does not show any light-emitting effect. Only the fibers with europium shell have a strong red light-emitting behavior.

## Materials and experimental methods

### Materials and instruments

A stainless steel coaxial needle purchased from Rame-Hart Instrument Inc., Succasunna, New Jersey, was used as the spinneret for the electrohydrodynamic co-casting experiment. The inner part was a needle with a gage size of 20. The outer needle had a gage size of 16. The PAN polymer with an approximate molecular weight of 150,000 was obtained from Scientific Polymer Products, Inc., Ontario, New York. Other chemicals including dimethylformamide (DMF), benzoic acid (BA), 1,10-phenanthroline (phen), and europium nitrate hexahydrate (all in the ACS purity) were purchased from Alfa Aesar, Ward Hills, Massachusetts. DMF was the solvent for making the PAN polymer solution. The black iron oxide ($Fe_3O_4$, molecular weight of 231.61) nanoparticle with an average size of 300 nm was purchased from Alpha Chemicals, Cape Girardeau, Missouri, USA. A high-voltage direct current power source was supplied by Spellman, Inc. Hauppauge, New York. A Fusion 200 precision syringe pump was purchased from Chemyx, Inc., Stafford, Texas. A model UVL-21 Compact UV lamp 4 W 365 nm, made by UVP in Upland, CA was used as the light source for red light-emitting tests. A PS-2600 Spectrometer and Fluorimeter, supplied by Pasco Scientific in Roseville, CA was used to test the fluorescence behavior of the EHD co-cast fibers.

### Fiber processing

Two solutions (I and II) were made for the electrohydrodynamic (EHD) co-casting experiments. Solution I refers to the Eu(BA)$_3$phen/PAN (PAN = polyacrylonitrile, phen = 1,10-phenanthroline, $C_{12}H_8N_2 \cdot H_2O$ with formula weight = 198.23, and BA = benzoic acid, $C_7H_6O_2$ with formula weight = 122.12). The basic composition of the $Eu^{3+}$ complex, Eu(BA)$_3$phen, was adopted from the literature [17, 18]. Solution II is described as $Fe_3O_4$/PAN. Solution I was made through the following procedures. First, 0.112 g europium nitrate hexahydrate, Eu(NO$_3$)$_3 \cdot$6H$_2$O,

with the formula weight = 446.06, 0.095 g benzoic acid, and 0.05 g 1,10-phenanthroline was dissolved into 9.0 mL of DMF in a 25.0-mL beaker. Then, 1.00 g PAN was added into the same beaker. After stirring at 60 °C for 30 min, the first solution, Solution I was obtained. The concentrations for the $Eu^{3+}$, benzoic acid (BA), and 1,10-phenanthroline (phen) in the polymer solution are 25.1, 77.8, and 25.2 mM, respectively. The second solution, Solution II, was made by mixing 0.058 g $Fe_3O_4$ nanoparticles with 1.00 g PAN in 9.0 mL DMF. The concentration of iron oxide is about 25.1 mM. The syringes shown in Fig. 1 were used to hold the two solutions separately. Electrohydrodynamic (EHD) co-casting Eu-containing shell solution (Solution I) and Fe-containing core solution (Solution II) was performed by using the coaxial needle. The injection rate of the syringe pump was set as 0.01 mL/min for both the sheath and core fluids. The power supply was turned on and set to 15 kV so that the electric field intensity was kept about 1.5 kV/cm. The nanofibers produced were collected on a soft tissue paper towel as the collector, which is about 10 cm away from the tip of the coaxial injection nozzle as illustrated in Fig. 1. For comparison, electrohydrodynamic (EHD) co-casting of Fe-containing shell solution (Solution II) and Eu-containing core solution (Solution I) was also performed using the same-sized coaxial needle, which generates long and uniform fibers as well. To examine the effect of europium content on the photoluminescence property, three other $Eu^{3+}$ complex solutions similar to Solution I, but with the different concentrations of 250, 10, and 2.5 mM were made for comparative studies. The names of these three solutions are given as follows: Solution $I_1$ stands for the one with 250 mM $Eu^{3+}$, Solution $I_2$ represents the one with 10 mM $Eu^{3+}$, and Solution $I_3$ is the one with 2.5 mM $Eu^{3+}$.
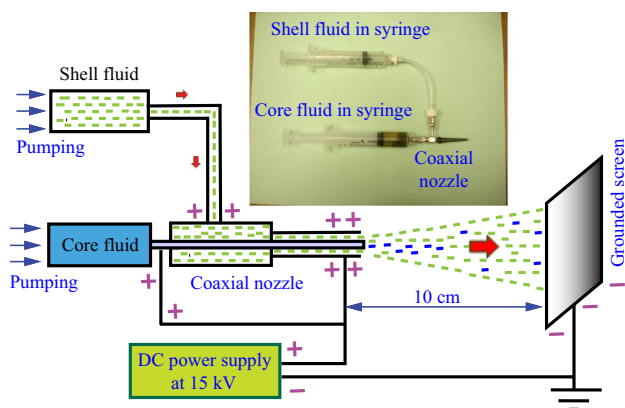


**Fig. 1** Schematic photo showing the electrohydrodynamic co-casting instrument for fiber processing

## Characterization

A scanning electron microscope (SEM model: JEOL JSM-6010PLUS/LA) with an Oxford Instruments energy dispersive X-ray spectroscopy attachment was used to examine the microstructure and analyze the composition of the prepared fibers. A SONY DSC-W100 Cyber-shot camera was used to take pictures of the fiber specimens with and without the ultraviolet light illumination. The pictures were used to evaluate the fluorescence of the fibers. The PS-2600 Spectrometer and Fluorimeter was used to measure the intensity of fluorescence under the 405-nm UV light excitation. Different integration times were used to capture the data for comparative studies of the fluorescence behavior. In addition, the lifetime of fluorescence for the EHD co-cast fibers was also determined using the same model of spectrometer and fluorimeter. Based on the fluorescence lifetime data, bi-exponential fitting was carried out to obtain the time constant. The structure of the Eu(III) complex was studied as well.

## Results and discussion

### Morphology and composition

The morphologies of the two types of fiber mats made by EHD co-casting are shown first. From the two SEM images in Fig. 2a, b, it can be seen that the fibers co-cast by the Fe-shell and Eu-core fluids are oriented randomly. The size of the fibers ranges from several hundreds of nanometers to several microns. Occasionally, some doughnuts are found in Fig. 2a. This feature is due to the non-uniform injection of the iron oxide nanoparticles and the PAN polymer. Bead formation can be observed in some area in Fig. 2b at a higher magnification. This is another morphological feature associated with the heterogeneity of the PAN polymer in the DMF due to the existence of the $Fe_3O_4$ particle suspension. The iron oxide nanoparticles increased the viscosity of the solution. In the domain with lower iron oxide concentration, the viscosity of the solution is lower. The injection rate tends to increase. Therefore, the stretching of the fibers is not so uniform. This allows the beads to form. Such a behavior was also found in some other polymer systems as shown by Sun et al. [3]. It is believed that if the solution was too dilute locally to form continuous jets, then heavily beaded fibers were formed instead of uniform filaments. The chemical compositions of the fiber were analyzed by energy dispersive X-ray diffraction spectroscopy (EDS). Mapping of the selected areas was performed to generate the elemental information. The qualitative result for this fiber is shown in Fig. 2c. It can be seen from Fig. 2c that C, O, Fe, and Eu are the major elements in the fibers. The characteristic peaks

**(a)**    20 µm
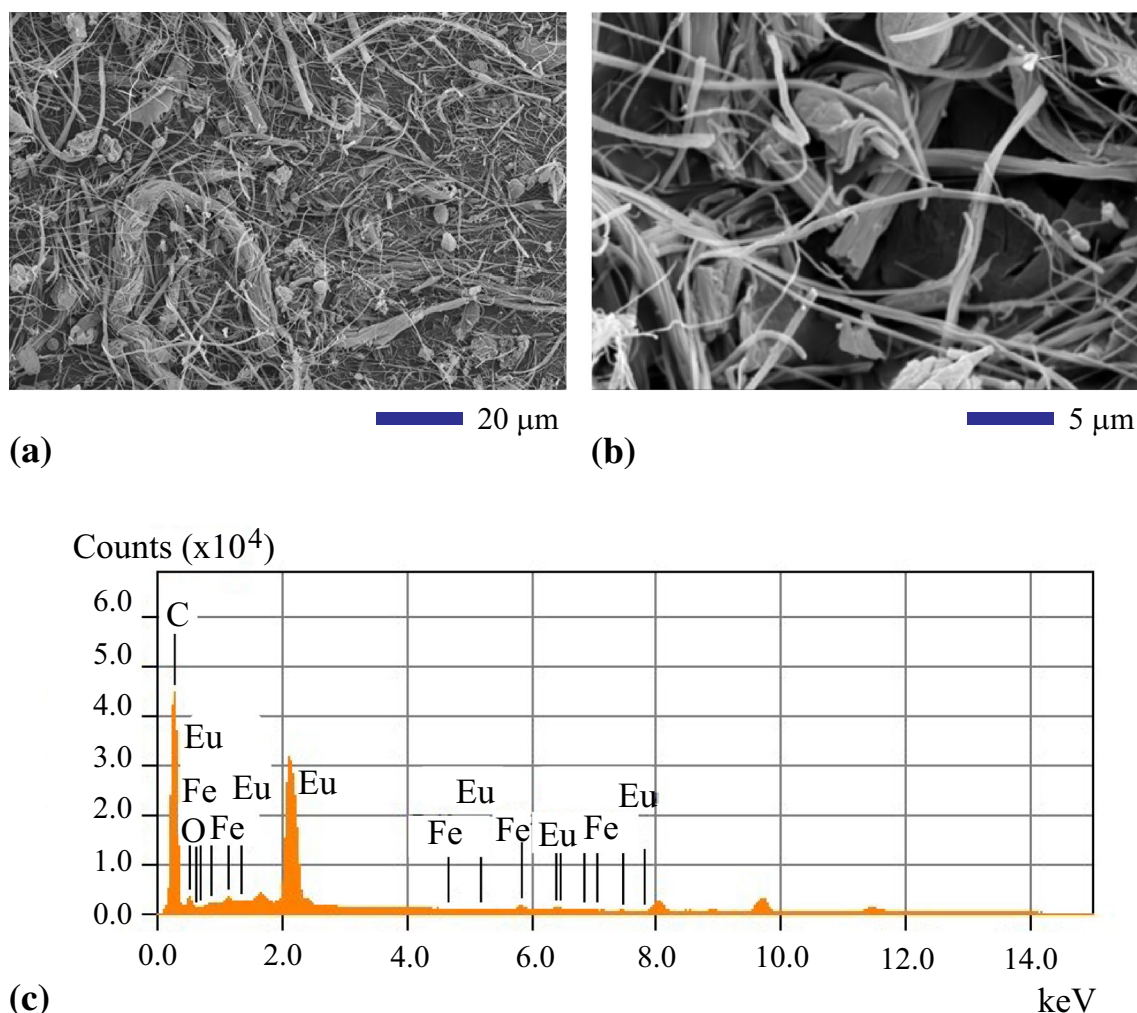


**(b)**    5 µm



**(c)**
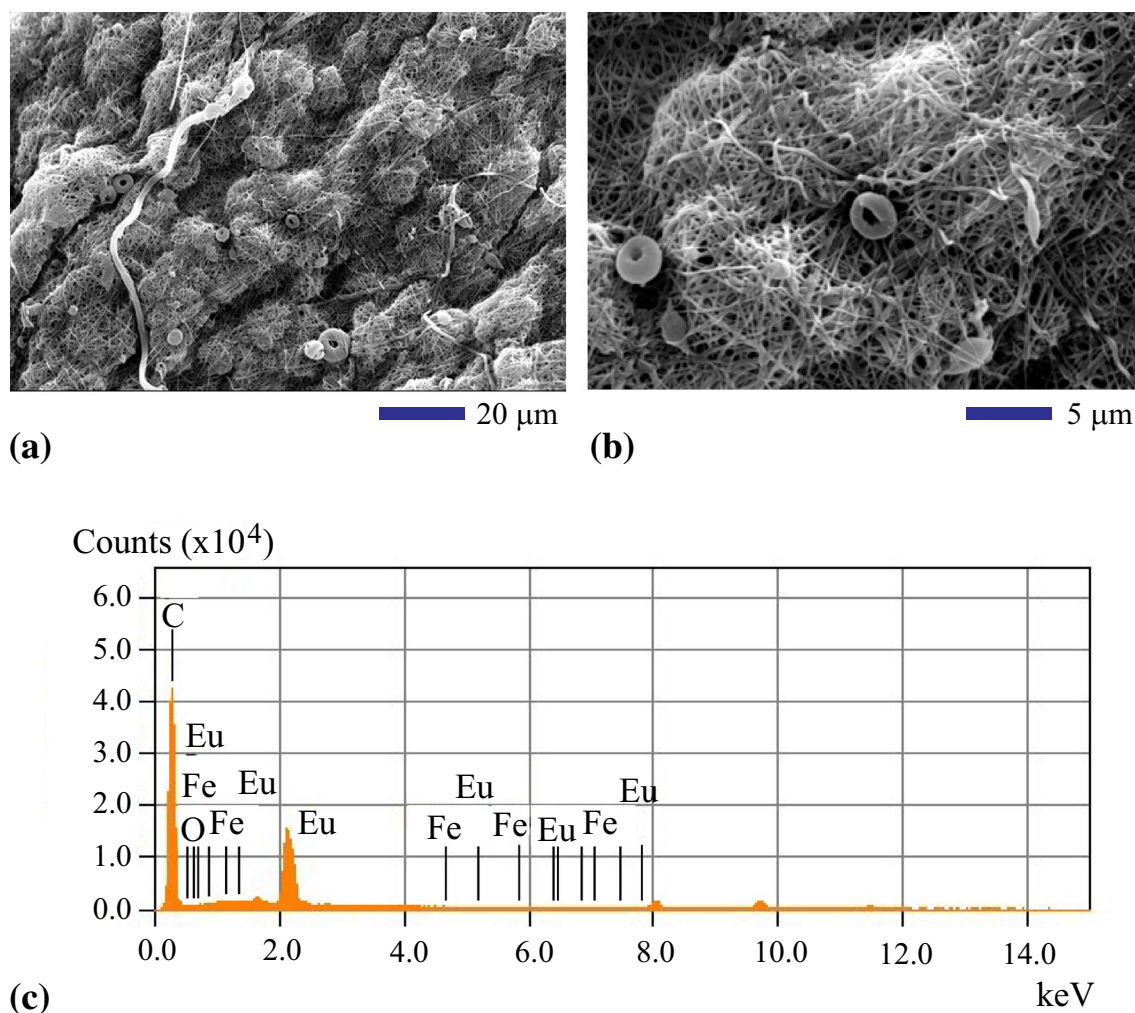
**Fig. 2** SEM analysis results of fibers made by electrohydrodynamic co-casting of the Eu-core fluid and Fe-shell fluid: **a** global view, **b** at a higher magnification, **c** energy dispersive spectrum

can be listed as follows: for iron, the $K_\alpha$ peak is located at 6.40 keV. $K_\beta$ peak is found at 7.06 keV. It can also be seen from the SEM/EDS the $L_{\alpha1}$ (0.71 keV), $L_{\alpha2}$ (0.60 keV), and $L_{\beta1}$ (0.79 keV) peaks. For europium, the major peaks including $L_\alpha$ (5.85 keV) and M (1.13 keV) are found. For oxygen, the $K_\alpha$ peak at 0.53 keV is seen. For carbon, the $K_\alpha$ peak is located at 0.28 keV.

It must be pointed out that the compositions of these fibers may also be measured through XPS apart from EDS. The X-ray photoelectron spectroscopy (XPS) technique also known as electron spectroscopy for chemical analysis (ESCA) is more widely used for surface analysis. It can be applied to various materials and generates quantitative and chemical state information from the surface of the samples examined. XPS instruments function in a manner analogous to SEM/EDS instruments that use a focused electron beam for compositional analysis. In contrast to SEM/EDS which has a typical analysis depth of 1–3 µm, XPS is a surface

analysis technique with a typical analysis depth of less than 5 nm. Obviously, XPS is better suited for the compositional analysis of ultra-thin samples. In this work, the fibers are in microscale sizes. Therefore, the SEM/EDS analysis is the preferred method for the compositional analysis.

Similarly, the SEM analysis of the fibers co-cast by using the Eu-shell and Fe-core fluids was made. Figure 3a shows a global view of the fibers. The fiber size changes a lot from micrometers to nanometers. Bundles of fibers are found in some regions. These fibers are in irregular shapes instead of the cylindrical shape as found for most core–shell nanofibers [4] or nanotubes [9, 10]. Pieces of bead-like materials are shown in Fig. 3b at a higher magnification. The chemical compositions of the fiber were analyzed by selected surface mapping and the energy dispersive X-ray diffraction spectroscopy (EDS) is shown in Fig. 3c. Again, the qualitative result revealed major elements of C, O, Fe, and Eu. The characteristic peak for oxygen is the $K_\alpha$ peak at

Fig. 3 SEM analysis results of fibers made by electrohydrodynamic co-casting of the Fe-core fluid and Eu-shell fluid: **a** global view, **b** at a higher magnification, **c** energy dispersive spectrum
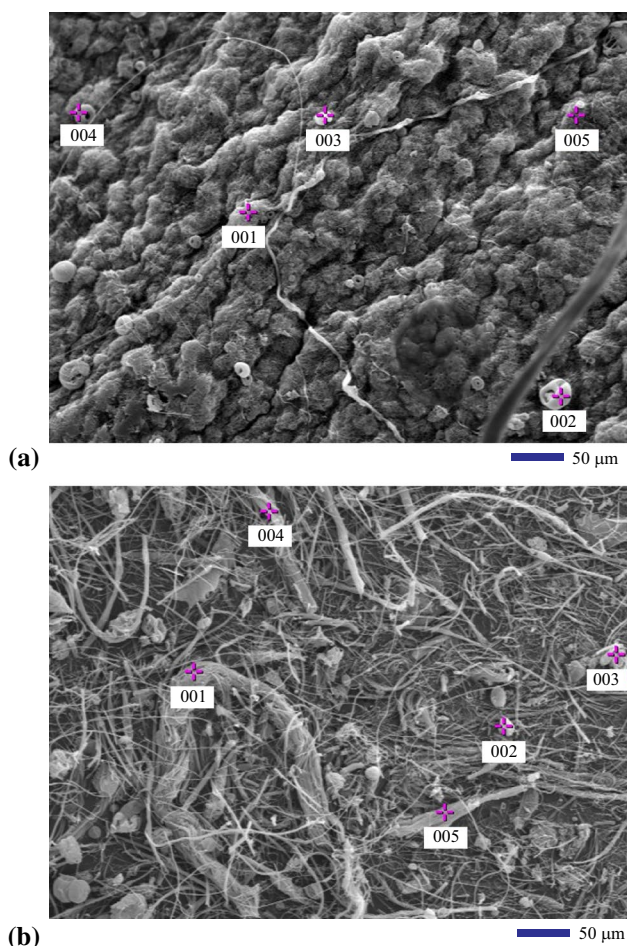
0.53 keV and the characteristic carbon emission is the $K_\alpha$ peak located at 0.28 keV. At least two europium peaks from the $L_\alpha$ (5.85 keV) and M (1.13 keV) emissions can be seen. More peaks for iron are found. These include the $K_\alpha$ peak located at 6.40 keV and $K_\beta$ peak at 7.06 keV. In addition, the $L_{\alpha1}$ (0.71 keV), $L_{\alpha2}$ (0.60 keV), and $L_{\beta1}$ (0.79 keV) peaks for iron are also shown.

Spot analysis was also performed to examine the uniformity of the chemical composition. The two SEM images in Fig. 4a, b provide the information of the spot locations at the two kinds of fibers. Figure 4a shows the five spot locations at the Fe-shell/Eu-core fibers, while Fig. 4b reveals the five spot locations at the Fe-shell/Eu-core fibers. The qualitative results of EDS are shown in Figs. 5 and 6 for the two fiber specimens. Such qualitative results from the spot analysis of five different spots indicate that there is no significant change in elemental types. The comparison of the height of peaks for the same

element (Eu) reveals the spreads. It is found that the Eu peak count at each subplot in Fig. 5 is lower than that shown in the corresponding subplot in Fig. 6. This indicates that the Eu peaks from the Eu-core@Fe-shell fiber are higher than those from the Fe-core@Eu-shell fiber. However, the electrohydrodynamically cast fibers are still fairly uniform in their chemical compositions.

The average values for the two kinds of fibers from the spot analysis are given in Table 1. From Table 1, it can be seen that C, O, Fe, and Eu are the major elements in the two fibers. The Fe-core@Eu-shell fiber shows a higher concentration of Eu than that of Fe. The atomic ratio of Eu to Fe is about 2:1. However, Eu concentration is much lower than the Eu element at the Eu-core@Fe-shell fiber. The atomic ratio of Eu to Fe is about 1:10. This is normal because the elements in the sheath layers can generate stronger signals than those in the core during the EDS measurements.

**(a)**                                                                          ▬ 50 μm



**(b)**                                                                          ▬ 50 μm

**Fig. 4** SEM images showing the locations for composition analysis: **a** fibers made from co-casting Eu-core fluid and Fe-shell fluid, **b** fibers made from co-casting Fe-core fluid and Eu-shell fluid

## Fluorescence and structure of the complex fiber

The fluorescence of the two types of fibers was tested under the excitation of UV light with a wavelength of 405 nm. Figure 7a, b shows the fluorescence results. The data shown in Fig. 7a were obtained from three runs. The repeated tests showed high repeatability of the acquired data. Obviously, the Eu-core@ Fe-shell fiber did not have any strong emission in the visible light spectrum range as illustrated in Fig. 7a. The reason for this behavior is that the Fe-shell layer generated strong shielding effect and completely blocked the UV light. In view of the concentration effect of iron oxide, a detailed study can be found in [18]. The higher concentration of iron oxide may be helpful for obtaining stronger magnetic response, which is meaningful for designing both fluorescence and magnetic field sensitive bi-functional fiber materials as discussed by Ma et al. [18].

Nevertheless, the Fe-core@Eu-shell fiber shows three emission peaks as marked in Fig. 7b. These three peaks are located at the wavelengths of 540, 580, and 610 nm. It was reported that there are three characteristic emission peaks of $Eu^{3+}$ under UV light excitations, i.e., $^5D_0 \rightarrow {}^7F_0$ (581 nm), $^5D_0 \rightarrow {}^7F_1$ (592 nm), and $^5D_0 \rightarrow {}^7F_2$ (617 nm) [17, 18]. With the hypersensitive transition at 617 nm, it became the dominant emission peak [17]. From Fig. 7(b), we noticed that the 610 nm peak has a wavelength range from 600 to 620 nm. It is corresponding to the dominant emission peak of the $Eu^{3+}$ at 617 nm.

The effect of integration time on the fluorescence of the Fe-core@Eu-shell fiber was investigated. Four integration times, 250, 500, 750, and 1000 ms, were used to do the data acquisition. The four datasets are plotted in Fig. 7b. It can be seen that increasing the integration time resulted in slight increase in the intensity of the fluorescence, but the three characteristic peaks remain unchanged.

The structure evolution is proposed following several steps as shown in Fig. 8. The three steps are applicable for the complex structure formation. In the first step as shown in Fig. 8a, the major composition in the europium nitrate hexahydrate, $Eu(NO_3)_3$, allowed the formation of $Eu^{3+}$ ion in the polar solvent of DMF. In the second step, the addition of the 1,10-phenanthroline and benzoic acid resulted in the coordinate complex formation as shown in Fig. 8b. Earlier studies also showed the coordination complex formation of Eu(III) with 1,10-phenanthroline and other acids or compounds [23, 24].

The electrohydrodynamic co-casting with PAN in DMF caused the evaporation of solvents and moieties including water, $HNO_3$, and DMF. This final step as shown in Fig. 8c allowed the complex attached to the PAN fiber through the coupling of the nitrogen on the PAN molecule and the $Eu^{3+}$ in the complex.

## Photosensitive behavior

To demonstrate the potential applications of the prepared core–shell fiber materials, photosensitivity test results are shown in Figs. 9 and 10. The results in Fig. 9 show the comparison of the photoluminescence behavior of the two fiber mats. Before any UV light excitation, the picture in Fig. 9a shows what the two fiber mats are like. With the 365 nm UV light excitation using the 4 W model UVL-21 Compact UV lamp, the Fe-core@Eu-shell fiber shows red light emission, but the Eu-core@ Fe-shell fiber shows the complete absorption of the light. The reason for such behavior can be explained as follows:

Iron oxide is an *n*-typed semiconductor [25]. Electron–hole ($e^-$-$h^+$) pair generation can be promoted by photon excitation. However, the charge recombination is faster than most of other semiconducting materials such as Si [26]. Therefore, the quick recombination of charges would not

**Fig. 5** X-ray diffraction energy dispersive spectra obtained from spot analysis of fibers made by electrohydrodynamic co-casting of the Eu-core fluid and Fe-shell fluid: **a** Spot 001 as shown in Fig. 4a. **b** Spot 002 as shown in Fig. 4a. **c** Spot 003 as shown in Fig. 4a. **d** Spot 004 as shown in Fig. 4a. **e** Spot 005 as shown in Fig. 4a
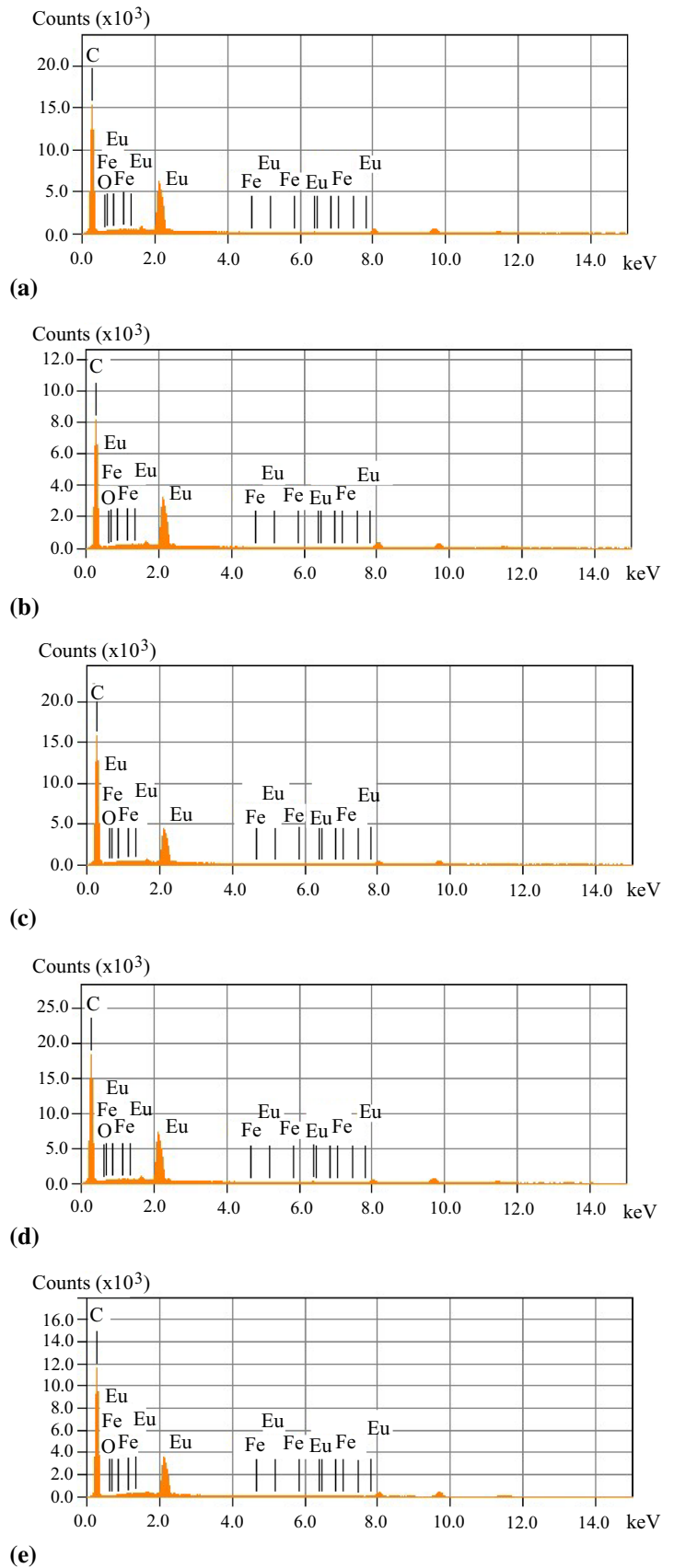
**Fig. 6** X-ray diffraction energy dispersive spectra obtained from spot analysis of fibers made by electrohydrodynamic co-casting of the Fe-core fluid and Eu-shell fluid: **a** Spot 001 as shown in Fig. 4b. **b** Spot 002 as shown in Fig. 4b. **c** Spot 003 as shown in Fig. 4b. **d** Spot 004 as shown in Fig. 4b. **e** Spot 005 as shown in Fig. 4b
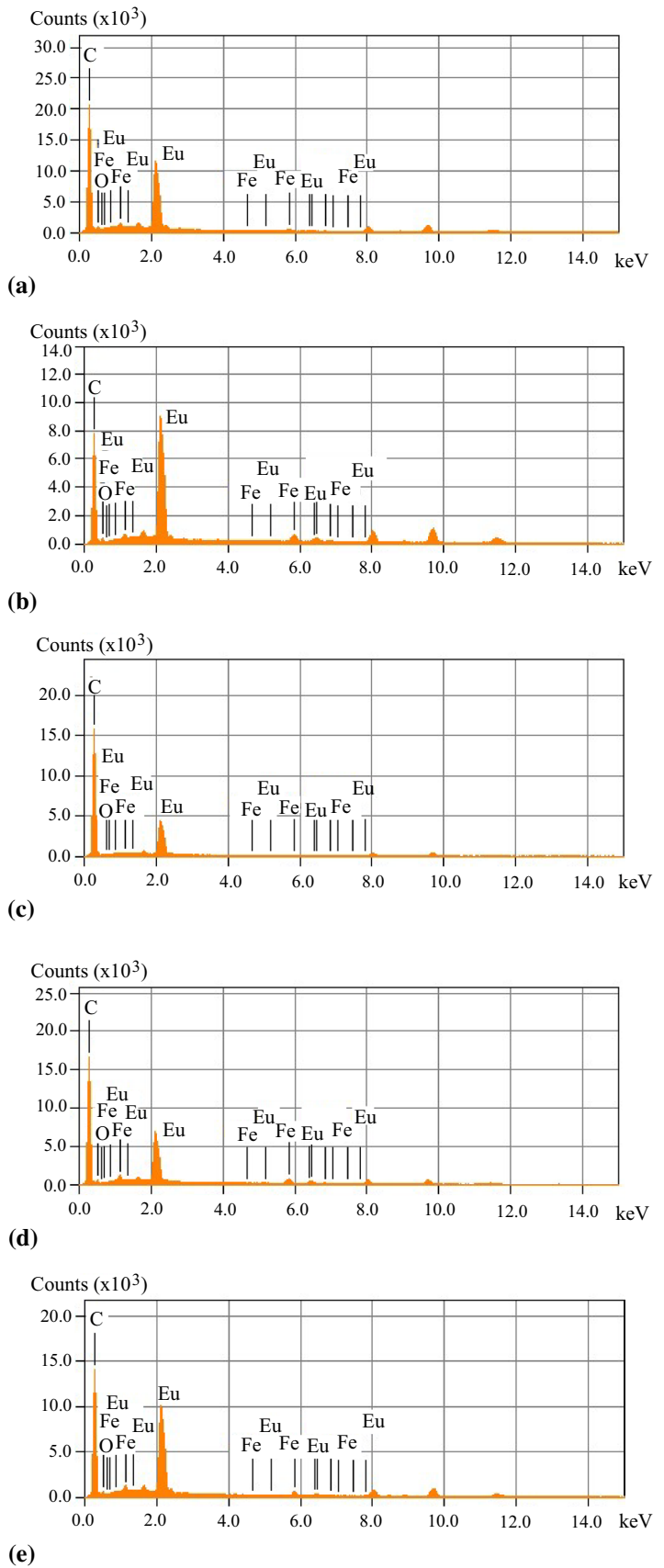
**Table 1** Chemical compositions of the two fibers measured by EDS

| Type of fiber | Content of element (atom%) | | | |
|---|---|---|---|---|
| | C | O | Fe | Eu |
| Eu-shell/Fe-core | 84.18 | 15.04 | 0.25 | 0.53 |
| Fe-shell/Eu-core | 93.91 | 5.88 | 0.2 | 0.02 |
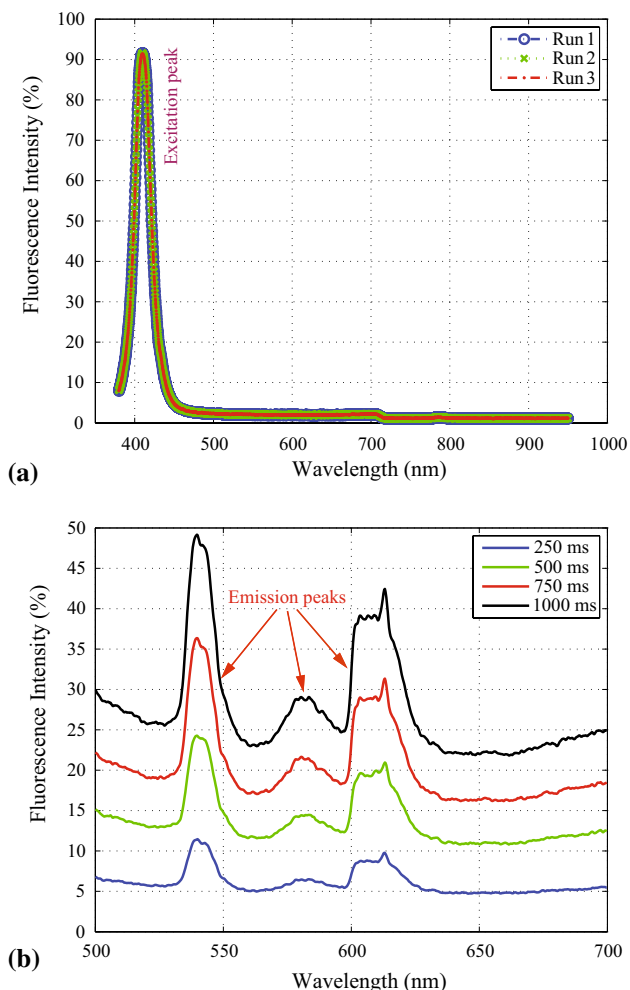


**Fig. 7** Photoluminescence of the two fibers under the 405 nm UV light excitation: **a** the Eu-core@Fe-shell fiber tested with three repeated runs, **b** the Fe-core@Eu-shell fiber tested using different integration time

allow the Fe-shell fiber to show any meaningful photoluminescence behavior.

In Fig. 10, the two photos show more details in the light emission of the Fe-core@Eu-shell fiber strands. Before the UV light excitation, the Fe-core@Eu-shell fiber setting on the soft paper substrate is shown in Fig. 10a. The Fe-core@Eu-shell fiber is white under visible light. Upon excitation by the 365-nm UV light, strong red light emission was observed. The fiber strands marked with an upper side down

arrow in both Fig. 10a, b are clearly revealed due to the intensive red light emission.

The intensive red light emission of the Eu-shell fiber comes from the two of the three emission peaks of Eu. The two peaks are identified at the wavelengths of 592 and 617 nm. The 592 nm emission peak belongs to the $^5D_0 \rightarrow {}^7F_1$ transition [17]. The $^5D_0 \rightarrow {}^7F_2$ transition generated the 617 nm peak [18]. The hypersensitive transition at 617 nm should be the dominant emission peak [17]. Such an intensive red light emission behavior of the Eu-containing micro- and/or nanofibers is useful for a lot of important applications including chemical sensors, bio-imaging probes, road flares, and photo sensors.

## Europium concentration effect

To study the $Eu^{3+}$ concentration effect on the photoluminescence behavior of the nanofibers, EHD co-casting Solution $I_1$ and Solution II was performed. Then, co-casting Solution $I_2$ and Solution II was done. Finally, Solution $I_3$ and Solution II are co-cast. Comparative studies on the four fibers with the $Eu^{3+}$ complex concentrations of 250, 25, 10, and 2.5 mM were made in view of the fluorescence intensity. Fluorescence tests on the four fibers with different europium concentrations were under the same conditions using the same 405-nm UV source. The same integration time was used to compare the intensity of the fluorescence. The results are shown in Table 2. It is found that higher the concentration of $Eu^{3+}$, the stronger is the fluorescence of the fiber. The fiber made from Solution $I_1$ with the highest $Eu^{3+}$ concentration of 250 mM and Solution II shows the highest relative intensity of 90.81%. When the $Eu^{3+}$ concentration drops ten times to 25 mM, the relative fluorescent intensity of the fiber made from Solution I with Solution II is reduced to 47.92%. Further reduction in the $Eu^{3+}$ concentration to 10 mM (Solution $I_2$) results in the relative fluorescent intensity of the fiber to 20.65%. The fiber made by co-casting the 2.5 mM $Eu^{3+}$ solution (Solution $I_3$) and Solution II has the lowest intensity of 3.24%. The concentration effect study provides a guideline on how high the $Eu^{3+}$ concentration should be to generate meaningful photoluminescence. From this study, the recommended concentration $Eu^{3+}$ for any useful optical sensing is 25 mM.

## Time-dependent fluorescence and lifetime measurement

To estimate the lifetime of the fluorescence, the time-dependent behavior was characterized using the fiber made from the Solution I (25 mM $Eu^{3+}$) and Solution II. The excitation wavelength of the UV light is still 409 nm. The intensity of fluorescence versus the time data were recorded and plotted in Fig. 11. The fluorescence data taking rate is 10 data/s. Totally
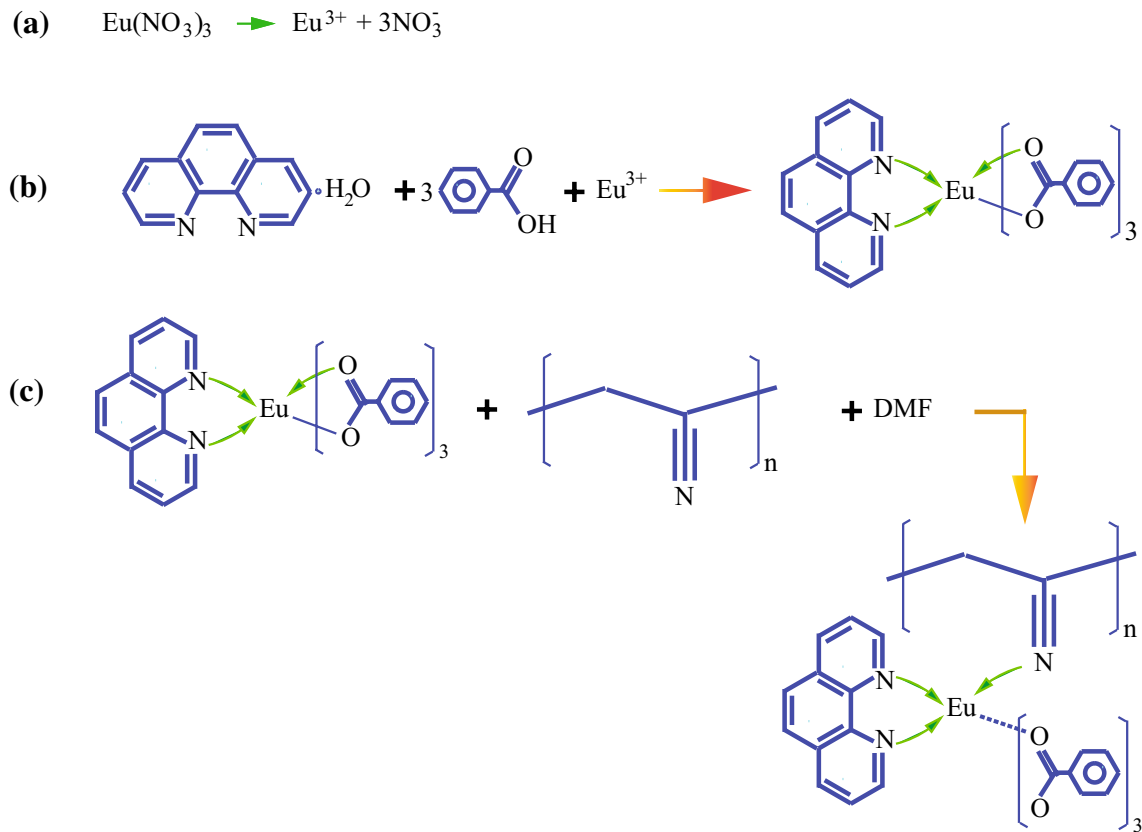
**Fig. 8** Structure development of the red light emission fiber: **a** Eu(III) ion formation, **b** Eu(III) complex formation, **c** Eu(III) complex attached to the PAN fiber

6129 sets of data were taken to generate the data plot as shown in the plot. The decaying in the fluorescence intensity was observed in Fig. 11. It can be divided into two stages. The first stage lasts about 2000 s and it is characterized by a relatively fast decaying mode. The intensity of fluorescence decreases linearly. The second stage reveals a slow decaying behavior. When the time elapses 2000 s, the intensity drops slowly. It takes several hours for the fluorescence to die out completely. The complete datasets are not shown in Fig. 11 for simplicity.

In view of the data fitting, a bi-exponential processing MATLAB code was written and the related constants were extracted. Basically, we assume that the fluorescence of the fiber follows a decaying pattern which can be characterized by two terms. The second term mainly catches the transient behavior of the photon emission, while the first term represents the steady state behavior of the fluorescence of the fiber.

The following formula was used to describe the trend of time-dependent fluorescence. The intensity fluorescence, $I$, is expressed by the following equation:

$$I = C_1 e^{-\alpha t} + C_2 e^{-\beta t}, \tag{1}$$

where $C_1$, $C_2$, $\alpha$, and $\beta$ are constants. Specifically, $\alpha$, and $\beta$ are related to the time constants characteristic of the fluorescence decaying.

Based on the data presented in Fig. 11, the four constants were obtained as $C_1 = 42.8178$, $C_2 = 7.4254$, $\alpha \rightarrow 0$, and $\beta = 0.0001$. The time constant, $\tau$ (with the unit of second), is calculated by:

$$\tau = \frac{1}{\beta} \tag{2}$$

The data fitting yields:

$$I = 42.8178 + 7.4254 e^{-0.0001t} \tag{3}$$

Therefore, the time constant from the data fitting formula of Eq. (3) is found to be 10, 000 s, which is over 3 h. Such a slow decaying property is required for specific applications including cell-labeling, bio-imaging, radioactive isotope detecting, and road flaring. Change in the integration time was also carried out. It is noted that such changes would not affect the extracted lifetime significantly. Although the fluorescent level increases with the increase in the integration time, the time constant for the fluorescent decaying is still around 10,000 s.
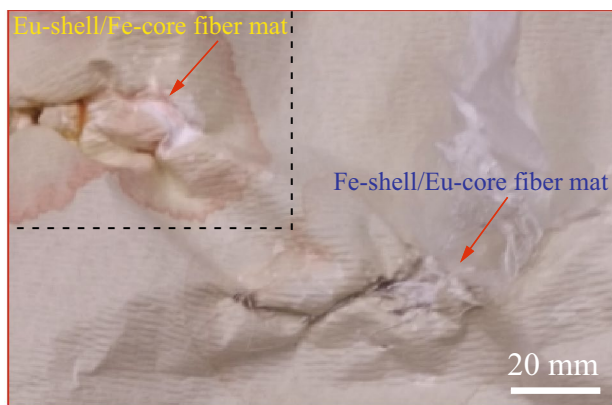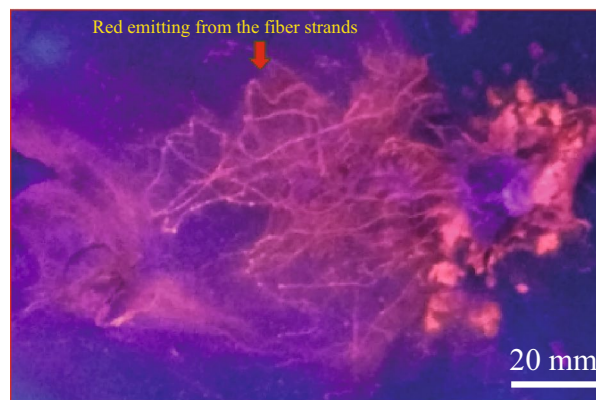
**(a)**
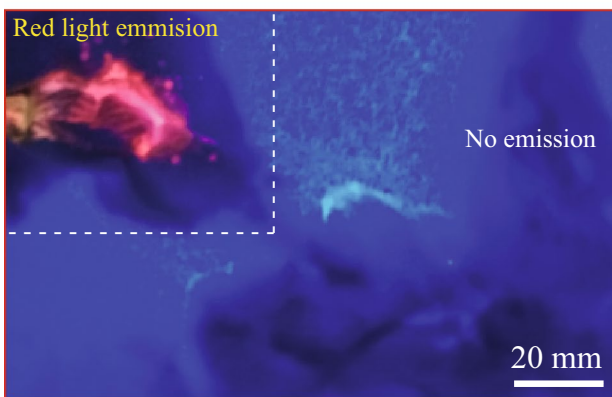


**(b)**

Fig. 9 Comparison on the photoluminescence between the two fiber mats: **a** without UV light excitation, **b** with the UV light excitation



**(a)**



**(b)**

Fig. 10 Photographs showing light emission of the Fe-core@Eu-shell fiber: **a** under visible light illumination, **b** with the strong red light emission due to the UV light excitation

## Conclusions

$Eu^{3+}$ organic complex was mixed with PAN-DMF solution in this work. The mixture solution was electrohydrodynamically co-cast with an iron oxide-containing PAN polymer solution into two different core–shell fibers successfully. The iron oxide may serve as the magnetic responsive component for obtaining dual functions of both fluorescence and magnetic field sensitive. The fiber with europium shell has a strong red light-emitting behavior. But the fiber with an iron oxide-containing shell does not show any ultraviolet light sensitivity. It is found that higher the concentration of $Eu^{3+}$, the stronger is the fluorescence of the fiber. The fiber made from Solution $I_1$ with the highest $Eu^{3+}$ concentration of 250 mM and Solution II shows the highest relative intensity of 91%. When the $Eu^{3+}$ concentration drops ten times to 25 mM, the relative fluorescent intensity of the fiber made from Solution I with Solution II is reduced to 47.92%. The decaying in the fluorescence shows two different stages. The first stage lasts about 2000 s and it is characterized by a fast

Table 2 Effect of $Eu^{3+}$ concentration in the sheath fluid on the fluorescence of the fibers

| $Eu^{3+}$ concentration in sheath fluid | 2.5 mM | 10 mM | 25 mM | 250 mM |
|---|---|---|---|---|
| Relative intensity of fluorescence | 3.24% | 20.65% | 47.92% | 90.81% |

decaying model. The intensity of fluorescence decreases linearly. The second stage has a slow decaying feature. It takes over 3 h for the fluorescence to die out completely. Bi-exponential data fitting shows that the time constant for the decay of fluorescence is about 10,000 s. It is concluded that the fiber with the europium sheath outer layer may find various potential applications including chemical sensing, photoluminescence, fluorescence, phosphorescence, bio-marking, and photon sensing.
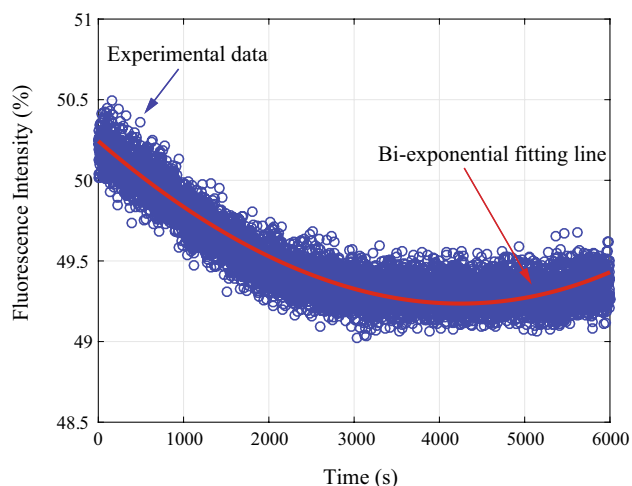
**Fig. 11** Time-dependent fluorescence intensity of the 25 mM $Eu^{3+}$ nanofiber under 405 nm UV light excitation

# References

1. Li, F., Zhao, Y., Song, Y.: Core-shell nanofibers: nano channel and capsule by coaxial electrospinning. In: Kumar, A. (ed.) nanofibers, vol. 22, pp. 419–438. Croatia, InTech (2010). ISBN 978-953-7619-86-2
2. Yarin, A.L.: Coaxial electrospinning and emulsion electrospinning of core–shell fibers. Polym. Adv. Technol. **22**, 310–317 (2011)
3. Sun, B., Duan, B., Yuan, X.: Preparation of core/shell PVP/PLA ultrafine fibers by coaxial electrospinning. J. Appl. Polym. Sci. **102**, 39–45 (2006)
4. Zhang, Y., Huang, Z.M., Xu, X., Lim, C.T., Ramakrishna, S.: Preparation of core-shell structured PCL-r-gelatin bi-component nanofibers by coaxial electrospinning. Chem. Mater. **16**(18), 3406–3409 (2004)
5. Zhang, Y.Z., Wang, X., Feng, Y., Li, J., Lim, C.T., Ramakrishna, S.: Coaxial electrospinning of (fluorescein isothiocyanate-conjugated bovine serum albumin)-encapsulated poly(ε-caprolactone) nanofibers for sustained release. Biomacromol **7**, 1049–1057 (2006)
6. Zhang, H., Zhao, C.G., Zhao, Y.H., Tang, G.W., Yuan, X.Y.: Electrospinning of ultrafine core/shell fibers for biomedical applications. Sci. China Chem. **53**(6), 1246–1254 (2010)
7. Chen, H., Zhao, Y., Song, Y., Jiang, L.: One-step multicomponent encapsulation by compound-fluidic electrospray. J. Am. Chem. Soc. **130**, 7800–7801 (2008)
8. Di, J., Chen, H., Wang, X., Zhao, Y., Jiang, L., Yu, J., Xu, R.: Fabrication of zeolite hollow fibers by coaxial electrospinning. Chem. Mater. **20**(11), 3543–3545 (2008)
9. Li, D., Xia, Y.: Direct fabrication of composite and ceramic hollow nanofibers by electrospinning. Nano Lett. **4**(5), 933–938 (2004)
10. Loscertales, I.G., Barrero, A., Marquez, M., Spretz, R.R., Velarde-Ortiz, R., Larsen, G.: Electrically forced coaxial nanojets for one-step hollow nanofiber design. J. Am. Chem. Soc. **2004**(126), 5376–5377 (2004)
11. Chan, K.H.K., Kotaki, M.: Fabrication and morphology control of poly(methyl methacrylate) hollow structures via coaxial electrospinning. J. Appl. Polym. Sci. **111**, 408–416 (2009)
12. Loscertales, I.G., Barrero, A., Guerrero, I., Cortijo, R., Marquez, M., Ganan-Calvo, A.M.: Micro/nano encapsulation via electrified coaxial liquid jets. Science **295**(5560), 1695–1698 (2002)
13. McCann, J.T., Marquez, M., Xia, Y.: Melt coaxial electrospinning: a versatile method for the encapsulation of solid materials and fabrication of phase change nanofibers. Nano Lett. **6**(12), 2868–2872 (2006)
14. Chen, H., Wang, N., Di, J., Zhao, Y., Song, Y., Jiang, L.: Nanowire-in-microtube structured core/shell fibers via multifluidic coaxial electrospinning. Langmuir **26**(13), 11291–11296 (2010)
15. Gan, Y.X., Chen, A.D., Gan, R.N., Hamdan, A.S.: Energy conversion behaviors of antimony telluride particle loaded partially carbonized nanofiber composite mat manufactured by electrohydrodynamic casting. Microelectron. Eng. **181**, 16–21 (2017)
16. Yu, J.H., Fridrikh, S.V., Rutledge, G.C.: Production of submicron diameter fibers by two-fluids electrospinning. Adv. Mater. **16**(17), 1562–1566 (2004)
17. Meshkova, S.B.: The dependence of the luminescence intensity of lanthanide complex with β-diketones on the ligand form. J. Fluoresc. **10**(4), 333–337 (2000)
18. Ma, Q., Yu, W., Dong, X., Wang, J., Liu, G., Xu, J.: Electrospinning preparation and properties of $Fe_3O_4$/Eu(BA)$_3$phen/PVP magnetic-photoluminescent bifunctional composite nanofibers. J. Nanopart. Res. **14**(10), 1203–1209 (2012)
19. Marchionna, S., Meinardi, F., Acciarri, M., Binetti, S., Papagni, A., Pizzini, S., Malatesta, V., Tubino, R.: Photovoltaic quantum efficiency enhancement by light harvesting of organo-lanthanide complexes. J. Luminescence **118**, 325–329 (2006)
20. Saha, A.K., Kross, K., Kloszewski, E.D., Upson, D.A., Toner, J.L., Snow, R.A., Black, C.D.V., Desai, V.C.: Time-resolved fluorescence of a new europium-chelate complex: demonstration of highly sensitive detection of protein and DNA samples. J. Am. Chem. Soc. **115**(23), 11032–11033 (1993)
21. Ouyang, X., Yu, R., Jin, J., Li, J., Yang, R., Tan, W., Yuan, J.: New strategy for label-free and time-resolved luminescent assay of protein: conjugate $Eu^{3+}$ complex and aptamer-wrapped carbon nanotubes. Anal. Chem. **83**(3), 782–789 (2011)
22. Choi, S.J., Persano, L., Camposeo, A., Jang, J.S., Koo, W.T., Kim, S.J., Cho, H.J., Kim, I.D., Pisignano, D.: Electrospun nanostructures for high performance chemiresistive and optical sensors. Macromolecular Mater. Eng. **302**(8), 1600569 (2007)
23. Mirochnik, A.G., Bukvetskii, B.V., Zhikhareva, P.A., Karasev, V.E.: Crystal structure and luminescence of the [Eu(Phen)$_2$(NO$_3$)$_3$] complex. The role of the ion-coactivator. Russ J. Coord. Chem. **27**(6), 443–448 (2001)
24. Biju, S., Ambili Raj, D.B., Reddy, M.L.P., Kariuki, B.M.: Synthesis, Crystal structure, and luminescent properties of novel $Eu^{3+}$ heterocyclic β-diketonate complexes with bidentate nitrogen donors. Inorg. Chem. **45**(26), 10651–10660 (2006)

25. Liu, H., Chi, D.: Synthesis of iron sulfide and iron oxide nanocrystal thin films for green energy applications. Procedia Eng. **141**, 32–37 (2016)

26. Rashid, N.M., Kishi, N., Soga, T.: Effects of nanostructures on iron oxide based dye sensitized solar cells fabricated on iron foils. Mater. Res. Bull. **77**, 126–130 (2016)

**Publisher's Note** Springer Nature remains neutral with regard to jurisdictional claims in published maps and institutional affiliations.

Springer